LIMITING DROP SIZE AND PREVAPORIZATION DEGREE REQUIRED FOR SPRAY DETONATION

S. M. Frolov, V. Ya. Basevich, and V. S. Posvianskii

N. N. Semenov Institute of Chemical Physics
Russian Academy of Sciences
Moscow, Russia

Introduction

Contrary to detonations in homogeneous gaseous mixtures, spray detonations encounter breakup and vaporization of liquid fuel drops, mixing of fuel vapor with air, and ignition of highly inhomogeneous partially premixed reactive gas followed by combustion of the heterogeneous medium. It is instructive to perform a comparative analysis of characteristic energy release rates at detonation of homogeneous and heterogeneous fuel–air mixtures of fixed fuel–air ratio and to determine a characteristic drop size (referred to as the 'limiting drop diameter') at which these rates are somewhat similar. Such an analysis would demonstrate how spray detonations are sensitive to drop size and initial fuel vapor content and would provide a road map for further improvement in the design of pulse detonation engine (PDE) prototypes.

This paper deals with the estimation of the limiting drop diameter for spray detonation. Evaporation and combustion of fuel drops was studied within the frame of the mathematical model [1, 2] providing surface regression rates and evolution of flame diameter consistent with available experimental data. The model considers a spherically symmetrical drop and neglects forced convection in both liquid and gas phases.

Autoignition and Combustion Chemistry

In [3–5], for modeling laminar and turbulent, premixed and nonpremixed combustion of n-alkane vapors in air, an efficient overall reaction mechanism containing eight reactions and seven species (C_nH_{2n+2}, O_2, H_2O, CO_2, CO, H_2, and generalized radical R) was developed and tested. However, as the flame propagation phenomena are different from autoignition, the rate constants of the rate-limiting reactions in this mechanism have to be modified to account for a slow initial stage of chain origination. The resultant overall reaction mechanism appli-

Table 1 Overall mechanism of n-alkane autoignition and combustion

No	Reaction	Heat effect H kcal/mol	A mol, l, s	m	E kcal/mol
1*	$C_nH_{2n+2} + (n + 0.5)O_2$ $= nCO + (n + 1)H_2$	535 ($n = 6$) 614 ($n = 7$) 1366 ($n = 16$)	$6.0 \cdot 10^{13}/p^{**}$ $7.0 \cdot 10^{14}/p^{***}$	0 0	50 50
2	$H_2 + H_2 + O_2$ $= H_2O + H_2O$	114	$7.0 \cdot 10^{13}/p^{0.5}$	0	21
3	$CO + CO + O_2$ $= CO_2 + CO_2$	134	$8.5 \cdot 10^{12}/p^{1.5}$	0	21
4	$H_2O + CO$ $= H_2 + CO_2$	10	$1.0 \cdot 10^{12}/p$	0	41.5
5	$H_2 + CO_2$ $= H_2O + CO$	−10	$3.1 \cdot 10^{13}/p$	0	49.1
6	$H_2O + M$ $= R + R + M$	−109	$2.8 \cdot 10^{17}/p$	−2	120
7	$R + R + M$ $= H_2O + M$	109	$9.5 \cdot 10^{12}$	−1	0
8	$R + O_2 + H_2$ $= R + R + R + H_2$	−4	$4.5 \cdot 10^{14}/p^{0.5}$	0.5	16.4

Remark: pressure p is taken in atm.

*Rate of reaction 1 is $W_1 = A_1 T^{m_1} \exp(-E_1/(RT))[C_nH_{2n+2}][O_2]$.

**For autoignition.

***For combustion.

cable to both autoignition and combustion of n-alkanes is presented in Table 1. In addition, heat effects of the first, rate-limiting reaction for n-hexane, n-heptane, and n-hexadecane — fuels considered in this paper — are presented. Note that, in general, the overall mechanism of Table 1 includes the dependence of the preexponential factor of the first reaction on the mixture equivalence ratio Φ. However, here this dependence is neglected and the values for $\Phi = 1$ are used.
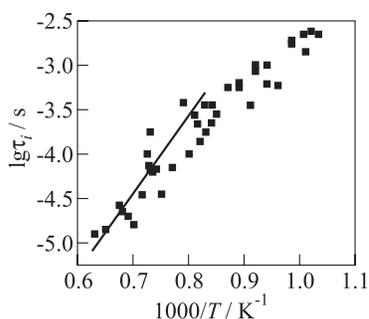

Figure 1 Comparison of predicted (curve) and available measured (symbols) ignition delay times for the stoichiometric premixed n-hexane–air mixture at a pressure of 15 atm

The autoignition delay times τ_i predicted based on this mechanism for the premixed stoichiometric n-heptane–air mixture at pressure of 15 atm are compared in Fig. 1 with available experimental data [5]. In the temperature range from 1100 to 1600 K, the agreement between the results is satisfactory. To validate the mechanism of Table 1 for autoignition of n-heptane drops, the predicted values of τ_i were compared with the experimental data [6, 7]. In the calculations, the initial drop and air temperatures were assumed to be spatially homogeneous and equal to 293 K and T_0, respectively. The size of the computational domain around the drop, R_m, was taken large as compared with the initial drop radius, r_0, so the parameters at the outer boundary of the computational domain

Table 2 Comparison of predicted and measured autoignition delay times for isolated n-heptane drops at a pressure of 1 atm

r_0, μm	T_0, K	τ_i, s	
		measured	predicted
350	1000	0.3 [6]	0.19
500	960	0.58 [7]	0.48

S. M. Frolov et al.

were kept constant during the computation. The results of the comparison are presented in Table 2 and can be treated as satisfactory. It is assumed that the autoignition kinetics of Table 1 are valid not only for n-heptane, but also for other n-alkanes. The indirect substantiation of this implication is the identity of the overall combustion mechanism for different n-alkanes up to C_{16} demonstrated in [3] based on the comparison of predicted and measured results for laminar premixed flames.

Limiting Drop Diameter for Spray Detonation

The limiting drop diameter for spray detonation is defined as the maximum drop size of dispersed liquid fuel which provides a similar heat-release rate behind the lead shock wave as is obtained for premixed fuel–air mixture of the same composition behind the shock wave of the same intensity. For estimating the limiting drop diameter, it is necessary to determine the evaporation and combustion time of drops of various initial sizes behind a shock wave. The estimates were made for the conditions behind a lead shock wave of the stoichiometric n-alkane–air detonation. The characteristic detonation velocity is 1800 m/s, and the characteristic values of pressure p_0 and temperature T_0 behind the lead shock wave are 30 atm and 1500 K, respectively.

According to numerous experimental observations of gaseous detonations, the characteristic time of chemical transformation behind the lead shock wave should not exceed a value of the order of 100 μs to ensure the self-sustaining propagation of a detonation. It is this approximate criterion that was used in the analysis below.

Isolated Drop. In the first series of calculations, an isolated fuel drop placed in the unconfined oxidizing atmosphere with $p_0 = 30$ atm and $T_0 = 1500$ K was considered. After a certain ignition delay time τ_i, autoignition occurs at some distance from the drop surface. Starting from this time, the maximum (flame) temperature starts to increase and after attaining a certain fixed value (taken equal to 2000 K), the kinetic mechanism of autoignition is replaced by the combustion mechanism; the values of parameters of the first (rate-limiting) reaction in Table 1 are replaced by the values relevant to the combustion process. Thus, after autoignition, the drop burns in a diffusion-controlled regime.
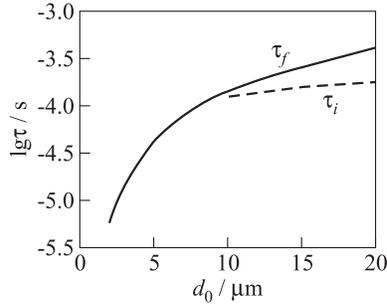
Figure 2 Predicted dependencies of ignition delay time, τ_i, and drop lifetime, τ_f, on the initial diameter d_0 of an n-hexane drop
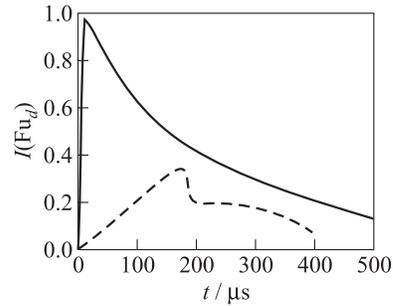
Figure 3 Predicted time histories of fuel index for n-hexane drops with $d_0 = 3$ μm (solid curve, $\tau_f = 13$ μs) and $d_0 = 20$ μm (dashed curve, $\tau_i = 180$ μs, $\tau_f = 410$ μs)

Figure 2 shows the typical predicted dependencies of the ignition delay time, τ_i, and drop lifetime, τ_f, on the initial drop diameter d_0. There is a clear trend: drop lifetime τ_f decreases faster with decreasing drop diameter than the ignition delay τ_i does.

Analysis of the results obtained indicates that at drop diameter $d_0 < 10$ μm, ignition fails even at large times due to evaporation-induced fast cooling of the gas adjacent to the drop surface and a resultant drastic decrease in the chemical activity near the drop. The whole range of drop diameters can be divided into two domains in terms of the relation between τ_i and τ_f. At large drop diameters, when $\tau_f > \tau_i$, a time available is sufficient for a spherical flame to form around the drop. In this case, the drop lifetime is determined by the diffusion-controlled combustion, i.e., $\tau_f \approx d_0^2/K$, where K is the combustion constant. At $\tau_f < \tau_i$, the concentrations of fuel vapor and oxidizer as well as temperature become nearly homogeneous in the computational domain and depend strongly on the domain size, R_m. At large R_m, the maximum temperature remains approximately equal to the initial temperature T_0 since evaporation of small drops is unable to decrease this temperature considerably and species concentrations decay rapidly with the distance from the drop.

S. M. Frolov et al.

To get an additional insight into the processes under consideration, introduce a time-dependent fuel index $I(\text{Fu})$ as the ratio of the fuel mass in the gas phase to the initial mass of the fuel drop:

$$I(\text{Fu}) = \int\limits_{r(t)}^{R_m} \frac{4\pi R^2 Y(t, R)\, dR}{4\pi r_0^3 \rho / 3}$$

where Y is the fuel mass concentration in the gas phase and ρ is the initial liquid fuel density.

Figure 3 shows the predicted time histories of the fuel index $I(\text{Fu}_d)$ for n-hexane drops with $d_0 = 3$ and 20 μm. Subscript "d" in the fuel index $I(\text{Fu}_d)$ means that fuel vapor originates from the drop to distinguish it from the fuel index $I(\text{Fu}_g)$ relevant to prevaporized fuel. When a drop evaporates without burning, the fuel index $I(\text{Fu}_d)$ tends to unity. When chemical reactions take place, the fuel index $I(\text{Fu}_d)$ tends to zero. Note that combustion products contain some amounts of CO and H_2; however, these amounts are usually small.

It follows from Fig. 3 that small drops 3 μm in diameter evaporate completely for a short time of $\tau_f \approx 13$ μs and then fuel vapor reacts slowly in almost isothermal conditions (with $T_{\max} \approx 1503$ K). At $t = 500$ μs, almost 13% of the fuel vapor remains unburned. Relatively large drops 20 μm in diameter do not evaporate completely before ignition. Ignition occurs at $t = \tau_i = 180$ μs and the drop burns rapidly and disappears at $\tau_f \approx 410$ μs. After drop disappearance, there is still about 6% of unreacted fuel vapor in the gas phase. Figure 3 indicates that both small and relatively large isolated drops react during a time interval that is considerably longer than a characteristic time of 100 μs available for reaction in a detonation wave.

Drop in a Spray. In the second series of calculations, a drop was surrounded by a spherical computational domain of size R_m such that the equivalence ratio inside this sphere corresponds to the overall mixture composition in the spray. The analysis is made for $\Phi = 1$. Configuration of the computational domain in this case describes approximately the behavior of a single drop in the monodisperse fuel spray [2]. Conventional boundary conditions for an isolated drop placed in an unconfined oxidizing atmosphere are not appropriate for this configuration.
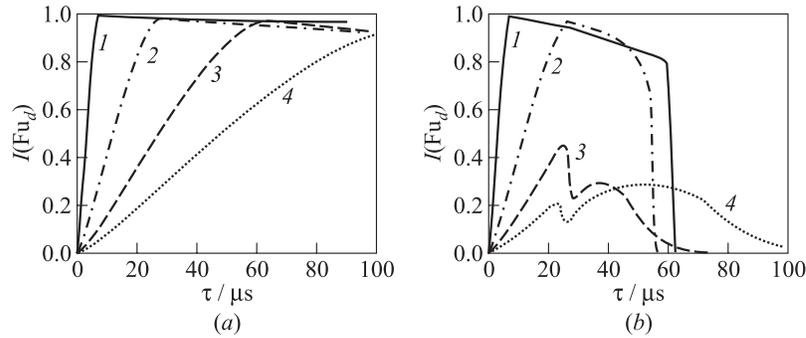
Figure 4 Predicted time histories of fuel index $I(\mathrm{Fu}_d)$ for small n-heptane drops with $d_0 = 2$ (*1*), 4 (*2*), 6 (*3*), and 8 μm (*4*). Gas-phase equivalence ratio Fu_g is equal to 0 (*a*), and 0.5 (*b*)

Therefore, the boundary conditions at the outer boundary of the computational domain encountered zero mass and energy fluxes and the boundary itself was made movable to ensure isobaric evolution of processes inside a sphere of initial radius R_m.

Figure 4a shows the time histories of fuel index $I(\mathrm{Fu}_d)$ for small n-heptane drops. Drops of initial diameter 2 μm evaporate in approximately 5.8 μs; however, chemical reactions are almost absent during the time of interest. This is caused by the average temperature decrease around the drop by about 300 K due to drop evaporation. The same is valid for drops 4, 6, and 8 μm in diameter.

Combustion is considerably accelerated if at the beginning of the process, the gas phase contains some amount of prevaporized fuel. This is illustrated in Fig. 4b, showing the predicted temporal dependencies of n-heptane fuel index at nonzero initial vapor content in ambient air, and in Fig. 5 for n-hexadecane drops. Parameter Fu_g denotes the initial equivalence ratio in the ambient atmosphere, so that curves with $\mathrm{Fu}_g = 0$ correspond to the case with no prevaporized fuel. Curves with $\mathrm{Fu}_g = 0.5$ correspond to the cases when the ambient atmosphere is the mixture of fuel vapor with air with the equivalence ratio of 0.5. The code used for the calculations allows tracing separately the fuel indices for the fuel vapor originating from the drop at $t > 0$ (denoted as $I(\mathrm{Fu}_d)$) and
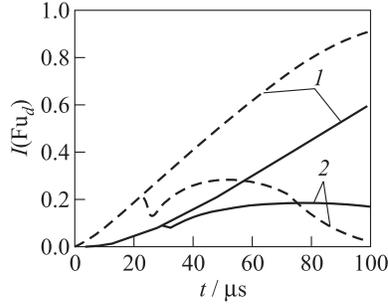
S. M. Frolov et al.

Figure 5 Predicted time histories of fuel index $I(\mathrm{Fu}_d)$ for n-heptane (dashed curves) and n-hexadecane (solid curves) drops of initial diameter $d_0 = 8$ μm. Gas-phase equivalence ratio Fu_g is equal to 0 (*1*) and 0.5 (*2*)
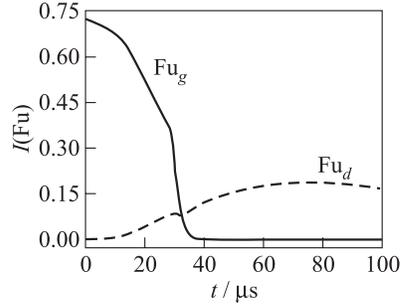
Figure 6 Predicted time histories of fuel indices $I(\mathrm{Fu}_d)$ and $I(\mathrm{Fu}_g)$ for n-hexadecane drop of initial diameter $d_0 = 8$ μm. Gas-phase equivalence ratio Fu_g is equal to 0.5

for the fuel vapor originating prior to the process due to prevaporization (denoted as $I(\mathrm{Fu}_g)$). In Figs. 4 and 5, the fuel index plotted along the Y-axis is $I(\mathrm{Fu}_d)$. Note that the total initial equivalence ratio Φ was always kept constant and equal to 1, i.e., in cases with $\mathrm{Fu}_g > 0$, the value of R_m has been changed correspondingly.

Clearly, at $\mathrm{Fu}_g > 0$ the rate of $I(\mathrm{Fu}_d)$ decay can change drastically starting from a certain time. For example, at $\mathrm{Fu}_g = 0.5$ (Fig. 4*b*), drops of initial diameter 6 μm exhibit fast decrease in fuel vapor concentration caused by ignition of initially prevaporized fuel at $t = \tau_i \approx 25$ μs. After ignition, the rate of fuel vapor depletion decreases due to transition to diffusion-controlled drop combustion. At $t = 80$ μs, fuel is completely burned. In the case of drops of initial diameter 8 μm, 4% of the fuel vapor remains unburned at $t = 100$ μs. Drops of initial diameter 2 μm ignite with $\tau_i \approx 60$ μs (strong cooling due to evaporation manifests itself), but completely burn out before 100 μs. The same qualitative features were observed in cases with $\mathrm{Fu}_g = 0.25$ and 0.75.

Less volatile n-hexadecane exhibits the trends that are similar to n-heptane; however, longer time is required as evident from Fig. 5. Ignition of n-hexadecane vapor occurs later than in the corresponding case

S. M. Frolov et al.   **117**

with n-heptane. At $t = 100$ μs, the concentration of n-hexadecane vapor attains a maximum value and drop still accumulates a large amount of liquid fuel. It is illustrated by Fig. 6, showing temporal evolution of both $I(\text{Fu}_d)$ and $I(\text{Fu}_g)$. When ignition occurs, both initial prevaporized fuel and newly evaporated fuel deplete simultaneously. However, while ignition results in almost complete burnout of prevaporized fuel, the fuel accumulated near the drop still has to burn in the diffusion flame.

Concluding Remarks

The results of calculations show that n-heptane drops of diameter 8 μm do not completely burn during 100 μs even if the ambient atmosphere has an equivalence ratio as high as 0.75, and therefore are not capable of supporting detonation in the n-heptane spray. In contrast, 6-micrometer n-heptane drops are capable of supporting the detonation if the amount of prevaporized fuel in ambient air provides the initial equivalence ratio of 0.5 in the gas phase. The same requirement should be met for 2-micrometer n-heptane drops. For 4-micrometer drops, the initial equivalence ratio of 0.25 in the gas phase is sufficient for detonation support. For n-hexadecane, all the requirements become more stringent and the detonation can be supported by smaller drops at higher prevaporization degrees. These results demonstrate that there exist definite requirements to the maximum drop size and the minimum prevaporization degree that have to be met to ensure detonation propagation in fuel sprays.

The estimates obtained here are substantiated by recent experimental findings [8]. It was shown in [8] that detonation in the stoichiometric mixture of JP-10 with air at initial pressure of 0.5 bar and initial temperature of 370 K can be obtained only with drops 3 μm in diameter and prevaporization degree of 75% (i.e., at $\text{Fu}_g = 0.75$). At $d_0 = 4$ μm and prevaporization degree of 25%, detonation failed. Unfortunately, a more accurate estimate of the limiting drop diameter and prevaporization degree cannot be made within the current approach as the "100-microsecond" criterion for detonation survival as well as the reaction mechanism applied are only approximate. Moreover, complex gasdynamic phenomena inherent in the shock–spray interaction have not been taken into account.

S. M. Frolov et al.

Acknowledgments

References

1. Frolov, S. M., V. Ya. Basevich, A. A. Belyaev, V. S. Posvianskii, and V. A. Smetanyuk. 2003. Detailed modeling of drop evaporation and combustion. In: *Combustion and atmospheric pollution*. Eds. G. D. Roy, S. M. Frolov, and A. M. Starik. Moscow, Russia: TORUS PRESS. 207–13.

2. Frolov, S. M., V. Ya. Basevich, A. A. Belyaev, V. S. Posvianskii, and V. A. Smetanyuk. 2004 (in press). Spray evaporation and combustion. Combustion and pollution: Environmental impact. Eds. G. D. Roy, S. M. Frolov, and A. M. Starik. Moscow, Russia: TORUS PRESS.

3. Evlampiev, A. V., S. M. Frolov, V. Ya. Basevich, and A. A. Belyaev. 2001. Overall kinetic mechanisms for modeling turbulent reactive flows. Part IV. Diffusion combustion. *Chemical Physics Reports* 20(11):21–27.

4. Basevich, V. Ya., S. M. Frolov, and A. A. Belyaev. 1998. Chemical mechanisms and the method of one-dimensional turbulent flame. *Chemical Physics Reports* 17(8):107–13.

5. Basevich, V. Ya., A. A. Belyaev, W. Branstaetter, M. G. Neuhaus, R. Tatshl, and S. M. Frolov. 1994. Kinetic scheme for modeling autoignition of *iso*-octane and *n*-heptane–air mixtures. *Combustion Explosion Shock Waves* 30(8–9):15–25.

6. Takei, M., H. Kobayashi, and T. Niioka. 1993. Ignition experiment of a blended-fuel droplet in a microgravity field. *Int. J. Microgravity Res. Appl. Microgravity Sci. Technol.* VI/3:184–87.

7. Niioka, T., H. Kobayashi, and D. Mito. 1994. Ignition experiment on droplet array in normal and microgravity environments. *IVTAM Symposium on the Mechanics and Combustion of Droplet and Sprays Proceedings*. Tainan. 367–77.

8. Brophy, C. M., D. W. Netzer, J. Sinibaldi, and R. Johnson. 2001. Detonation of a JP-10 aerosol for pulse detonation application. In: *High-speed deflagration and detonation: Fundamentals and control*. Eds. G. Roy, S. Frolov, D. Netzer, and A. Borisov. Moscow, Russia: Elex-KM Publ. 207–22.